

SHOT PEEN IMPACT ON LIFE, PART 3: DEVELOPMENT OF A FRACTURE MECHANICS / THRESHOLD BEHAVIOR PREDICTIVE MODEL

M. Tufft

General Electric Aircraft Engines, Cincinnati, Ohio USA

ABSTRACT

Shot peening, long recognized for its potential to increase fatigue life capability has also been observed to cause the reverse effect under some circumstances. Single particle impact tests resulted in two major observations: 1) increase in velocity correlated with a deviation from Hertzian impact behavior, and 2) as impact severity increased, so did accumulation of microstructural slip. These observations ultimately led to the development of a dual criteria Fracture Mechanics / Threshold Behavior fatigue life predictive model. This model, developed for René 88DT, permits a lower bound life estimate and can be used to help define robust peening conditions. A microstructural slip depth measurement is used to define an initial crack size for a Fracture Mechanics calculation, providing a lower-bound life estimate. An impact severity criteria, linked to total shot velocity, is used to identify conditions for which the Fracture Mechanics model life estimate is conservative.

KEYWORDS

Shot peening, fatigue damage, fracture mechanics, impact severity, shot velocity, microstructure development, damage prediction, René 88DT, conditioned cut-wire shot.

INTRODUCTION

Results from a designed experiment [1] indicated that shot peening can result in reduced fatigue life capability under some conditions. The fatigue process consists of four phases: 1) work hardening or work softening, 2) crack nucleation, 3) crack propagation and 4) final failure. The three most favorable crack initiation sites are: 1) slip bands, 2) grain boundaries, 3) inclusions [2]. The shot peening process induces changes in the surface layer of the workpiece material which can be broadly grouped into three categories: 1) microstructural changes, 2) build up of residual stresses, and 3) increase in surface

roughness due to dimple formation at impact. Shot peening plastically deforms the surface layer, although degree of saturation may depend on peening condition and coverage. Plastic deformation involves generation of dislocations; cyclic plastic deformation generates features such as persistent slip bands which are favorable crack nucleation sites. As a result, the shot peening process can create many potential crack initiation sites in the surface layer.

Single particle impact tests were conducted using production shot [3] to investigate material behavior under a variety of impact conditions. A change in impact response was observed above a certain velocity threshold, as was development of observable surface slip bands. As a result of these observations, it was hypothesized that the slip layer could represent a microstructural damage layer. If sufficient damage is localized, shot peening may complete the crack nucleation phase locally at various surface sites, resulting in life dominated by the crack propagation phase. In these cases, it should be possible to use a fracture mechanics model to provide a lower bound life estimate.

The peening conditions from the Bailey Designed Experiment [1] were replicated on flat coupons for further analysis, to assist with the development of a model for damage prediction. Specimens were weighed before and after peening to detect erosion. Chemical composition was evaluated using Auger spectroscopy and energy dispersive spectroscopy techniques before and after peening. Micrographs were made to reveal the microstructure below the peened surface. Residual stress profiles were generated for each of the DOE peening conditions using x-ray diffraction methods. Plastic strain accumulation was investigated using x-ray diffraction (line broadening) and TEM analysis of thin foils taken perpendicular to the surface. Surface roughness measurements were taken using both needle type profilometers (Tencor Alpha Step 200) and vertical scanning interferometers (WYKO RST plus). Toward the end of this effort, it was also possible to get velocity measurements for selected peening conditions using an electro-magnetic velocity sensor [4]. The information obtained from these analyses were used to formulate damage layer estimates, which were then evaluated using fracture mechanics predictions for the low cycle fatigue (LCF) specimen tests from the Bailey DOE.

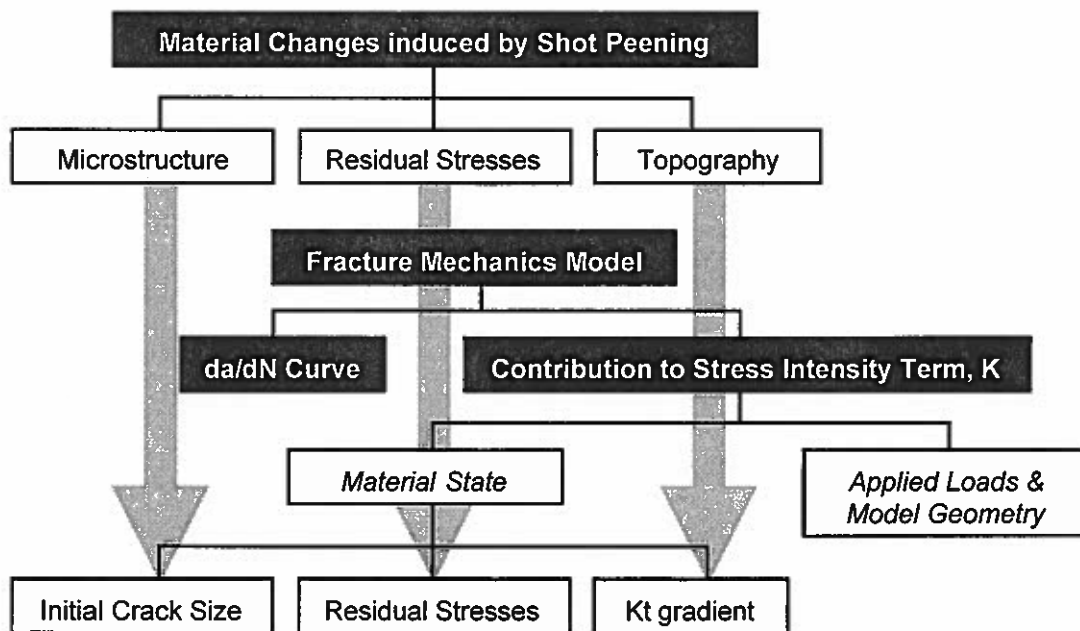


Figure 1: Development of the Fracture Mechanics Model

DEVELOPMENT OF A FRACTURE MECHANICS MODEL

Figure 1 illustrates how changes in material state induced by shot peening can be incorporated into a fracture mechanics model. This approach models the damage layer by an initial crack radius, and surface roughness by a surface stress concentration factor (K_t) incorporated into a stress gradient. Of these, determination of a damage layer depth is critical to the process, and the fundamental challenge. Incorporation of a stress concentration gradient did not improve the correlation and was eventually eliminated from the model. Modeling of shot peening residual stresses is a well established practice. The main caution is the need to calibrate the model with experimental data to account for the effects of residual stress relaxation and interaction with stress cycling effects. Since fracture mechanics is also a well established discipline, this paper will focus on aspects of the model unique to the shot peened damage prediction problem. Additional details of the fracture mechanics method used can be found in Tufft [4].

Initial Crack Size from Microstructure

Fracture surfaces from the Bailey test specimens [4] revealed oxidized semi-circular surface crack initiation sites for all "low" life results. The oxidation indicates an area which was exposed to oxygen significantly longer than the rest of the fracture surface at the 1000°F test temperature. These observations suggest that a semi-circular initial crack shape is adequate to model the failures observed. This reduces the problem to one dimension: how to define a crack radius.

Development of slip bands in the single particle impact tests [3] with increasing impact severity first suggested that slip bands might be related to microstructural damage. Microcracking observed on a model disk showed crack initiation formed along slip bands induced by shot peening, as shown in Figure 2. This further supports the concept of a damage layer linked to slip band formation in René 88DT. The main challenge is how to characterize this damage layer depth.



Figure 2 – SEM Backscatter Electron Image Showing Crack Formation Along a Slip Band (1.5 kX).

Slip depth was identified as the critical feature corresponding to an initial crack size in René 88DT. A rationale was needed for the specific slip depth measurement criteria. Conditioned cut wire shot impart a fairly uniform slip layer in the workpiece. Crack formation is known to occur in regions of high stress localization, i.e. high Kt region. So, a competition is likely to develop among the deepest dimples on the surface. The dimple having the most favorably oriented slip system (aligned with the shot impact vector and favorably oriented for shear) is likely to win. Regions with lower Kt's are likely to lose the competition, even if there is greater slip depth beneath the surface. From the surface roughness data [4], it was found that the Kt generally decreases with increasing coverage. However, slip depth was found to increase with increasing coverage. Thus it appears that a relative minimum slip depth will correspond to the crack initiation site for René 88DT targets peened with conditioned cut wire shot. This may also create a "plastic hinge" effect, resulting in a relatively weaker low slip region sandwiched between more highly work-hardened regions, creating a "weak link" for additional strain localization. For this effort, a minimum average slip layer depth measurement was generated from slip layer depth measurements at three different surface locations for use as an initial crack radius.

Residual Stresses

Residual stresses are readily measured using x-ray diffraction techniques. Based on prior work by VanStone [5], experience shows that good curve fits to residual stress profiles can be obtained by using a product of exponential and sine functions (see Figure 3).

$$\sigma_{RS}(x) = A_1 \cdot \exp[-x/\lambda] \cdot \sin(B_1 \cdot x + C_1) \quad (1)$$

Residual stress profiles were obtained from Lambda Research x-ray diffraction measurements, which were then curve fit using equation 1, as illustrated in Figure 3. The residual stress profile can then be incorporated into a fracture mechanics analysis using principles of linear superposition via a Green's function approach. Summaries of profiles & curve fit coefficients can be found in Tuftt [4]. Fuchs [6] observed a nearly linear relationship between shot peened intensity and the depth of the compressive stress layer, which was also observed for René 88DT as shown in Figure 4. Note that a small compressive stress layer is present in unpeened low stress ground and polished specimens.

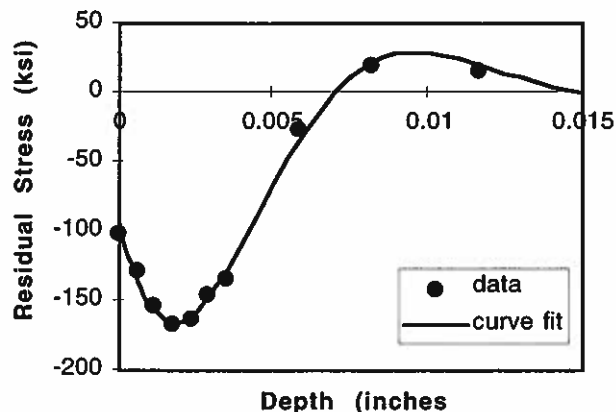


Figure 3 – Sample Residual Stress Profile and Corresponding Curve Fit
Peening condition: CCW31 shot, 6A intensity, 45° incidence angle, 800% coverage.

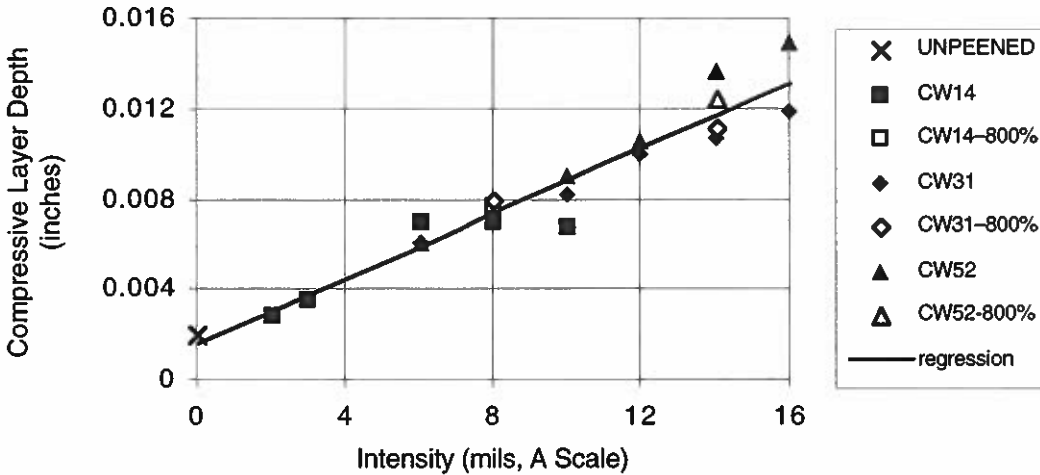


Figure 4 – Compressive Stress Layer Depth as a Function of Peening Intensity

K_t Gradient Definition from Topography

Work done by Li, Yao, Wang and Wang [7] established a method for estimating a K_t gradient due to multiple dimples or craters. Extensive 3D stress analysis was conducted and a formula for a K_t was extended for use with surface roughness data, as given below. R_{tm} represents a maximum peak height, and S represents an average spacing between features.

$$K_t = 1 + 4.0(R_{tm} / S)^{1.3} \quad (2)$$

To generate a K_t gradient, g(x), as a function of depth into the material, it is necessary to fit this to a curve. An exponential curve was used, with a decay depth corresponding to 3 times the characteristic distance, R_{tm}.

$$g(x) = (K_t - 1) \cdot \exp\left[-x / (3R_{tm})\right] + 1 \quad (3)$$

The decay depth of 3*R_{tm} was chosen because 1) the maximum peak height represents a distance characteristic of the surface roughness along the depth direction, and 2) in finite element analysis, it is commonly noted that localized effects due to application of boundary conditions decay away approximately three times a characteristic distance.

Surface roughness data were used to generate a K_t gradient for each condition, using equations 2 and 3. It was observed that cw31 shot results in a lower K_t at the same intensity. Near normal incidence angles resulted in lower K_t's than low incidence angles. For a given intensity and shot size, higher coverage resulted in a lower K_t. Additional details can be found in Tufft [4]. The stress concentration gradient due to dimple roughness did not turn out to be a significant factor for the fracture mechanics assessment and was not used in the final correlation. This could be due to: 1) extremely shallow depth of gradient, 2) local stress relaxation in the damage layer due to stress redistribution or microcracking as described in Zukas [8], or the conservative approach of modeling the slip layer as a crack.

Velocity Measurements for Production Peened Coupons

Velocity measurements for a subset of production peening conditions were obtained after the fracture mechanics model had been developed and correlated. Figure 5 illustrates the difference in velocity behavior as a function of intensity between shot sizes. Total velocities > 2,445 in/s (62 m/s) were observed for peening conditions resulting in "low" life conditions, which is consistent with the onset of slip and deviation from Hertzian behavior observed in the single particle impact tests [3] at velocities > 2,280 in/s (58 m/s).

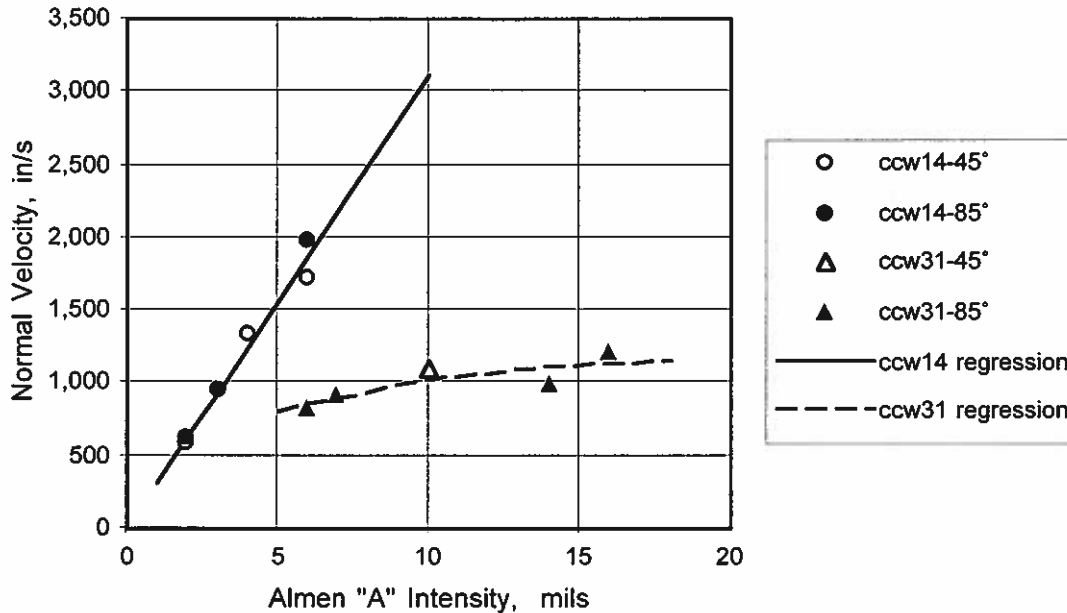


Figure 5 – Velocity as a Function of Intensity for Production Shot

FRACTURE MECHANICS / THRESHOLD BEHAVIOR MODEL

Table 1 provides a summary of selected results for life correlations with the sixteen DOE conditions in standard order, including information about shot peening conditions, life behavior, stress concentration factor (Kt) and initial crack size (a) measured from microstructural data. Life information is provided in a number of ways to facilitate comparisons with low cycle fatigue behavior as well as fracture mechanics-dominated behavior, including the parameters "stdev" (as defined in equation 1), "Nfm/Nobs", and "Nlcf/Nobs". "Nobs" is the observed life at failure, Nfm is the fracture mechanics model prediction. "Navg" or "Nlcf" is the average low cycle fatigue life, and " $N_{-3\sigma}$ " is the minimum "-3 σ " low cycle fatigue life for unpeened low stress ground and polished specimen tests. "Stdev" is used to represent a test life result in terms of the number of standard deviations from average low cycle fatigue capability for that condition, and is defined as:

$$stdev = \frac{\left[\log(N_{obs}) - \log(N_{avg}) \right]}{\left[\log(N_{avg}) - \log(N_{-3\sigma}) \right] / 3} \quad (4)$$

Figure 6 shows the data mapped in terms of "LCF" behavior and "FM" behavior regimes. Scatterbands of $\pm 2\sigma$ are provided on the "stdev" or LCF axis, while 2X scatterbands are provided on the "Nfm/Nobs" or FM axis.

Table 1 – Summary of Results

cond. #	Shot	Intensity	Incidence Angle	Coverage	Average stdev	Kt	a (inches)	Initiation Site	ACTUAL LIFE, Nobs	Predicted Life, Npred	FM prediction, Nfm	LCF prediction, Nicf	Npred/ Nobs	Nfm/ Nobs	Nicf/ Nobs	stdev
1	ccw14	6A	45	100%	0.06	1.29	0.0009	I	156,558	102,855	1,000,000	102,855	0.66	K<Kth	0.66	0.10
								I	126,779	92,607	1,000,000	92,607	0.73	K<Kth	0.73	0.03
2	ccw14	6A	45	800%	-3.62	1.18	0.0021	S	23,598	19,810	19,810	92,607	0.84	0.84	3.92	-3.83
								S	29,523	21,877	21,877	97,072	0.74	0.74	3.29	-3.42
3	ccw14	6A	85	100%	0.55	1.31	0.0005	I	163,647	95,248	1,000,000	95,248	0.58	K<Kth	0.58	0.55
								I	invalid test							
4	ccw14	6A	85	800%	-1.16	1.18	0.0014	I	134,393	88,607	88,607	92,607	0.66	0.66	0.69	0.16
								S	38,504	45,486	45,486	85,167	1.15	1.15	2.16	-2.47
5	ccw14	10A	45	100%	-3.44	1.48	0.0014	S	27,203	30,438	30,438	88,431	1.12	1.00	3.25	-3.41
								S	28,909	29,051	29,051	97,072	1.00	1.12	3.36	-3.47
6	ccw14	10A	45	800%	-4.19	1.47	0.0026	S	20,253	22,230	22,230	95,248	1.10	1.10	4.70	-4.23
								S	21,467	20,861	20,861	97,072	0.97	0.97	4.52	-4.15
7	ccw14	10A	85	100%	-0.89	1.33	0.0014	I	138,633	83,426	83,426	90,048	0.60	0.60	0.65	0.29
								S	49,529	72,501	72,501	90,048	1.46	1.46	1.82	-2.07
8	ccw14	10A	85	800%	-4.00	1.25	0.0025	S	21,621	22,784	22,784	97,800	1.05	1.05	4.52	-4.17
								S	22,311	38,432	38,432	87,043	1.72	1.72	3.90	-3.83
9	ccw31	6A	45	100%	0.32	1.25	0.0012	I	137,555	89,573	95,976	89,573	0.65	0.70	0.65	0.29
								I	141,969	89,371	71,039	89,371	0.63	0.50	0.63	0.36
10	ccw31	6A	45	800%	0.61	1.23	0.0013	I	141,026	95,248	91,076	95,248	0.68	0.65	0.68	0.21
								I	132,206	62,856	66,181	62,856	0.48	0.50	0.48	1.02
11	ccw31	6A	85	100%	0.14	1.17	0.0005	I	143,627	101,921	1,000,000	101,921	0.71	K<Kth	0.71	-0.05
								I	139,635	89,371	1,000,000	89,371	0.64	K<Kth	0.64	0.32
12	ccw31	6A	85	800%	0.28	1.12	0.0011	I	145,630	91,907	1,000,000	91,907	0.63	K<Kth	0.63	0.36
								I	126,348	85,167	1,000,000	85,167	0.67	K<Kth	0.67	0.20
13	ccw31	10A	45	100%	0.44	1.25	0.0010	I	142,725	86,978	900,000	86,978	0.61	stall	0.61	0.43
								I	151,554	92,607	900,000	92,607	0.61	stall	0.61	0.44
14	ccw31	10A	45	800%	0.36	1.23	0.0021	I	141,723	94,454	25,257	94,454	0.67	0.18	0.67	0.24
								I	150,913	90,048	26,901	90,048	0.60	0.18	0.60	0.49
15	ccw31	10A	85	100%	0.36	1.25	0.0018	I	143,340	90,048	25,334	90,048	0.63	0.17	0.63	0.37
								I	161,649	99,248	28,226	99,248	0.61	0.18	0.61	0.35
16	ccw31	10A	85	800%	0.20	1.23	0.0022	I	143,004	96,753	24,626	96,753	0.68	0.17	0.68	0.20
								I	invalid test							

I = internal initiation, S = surface initiation

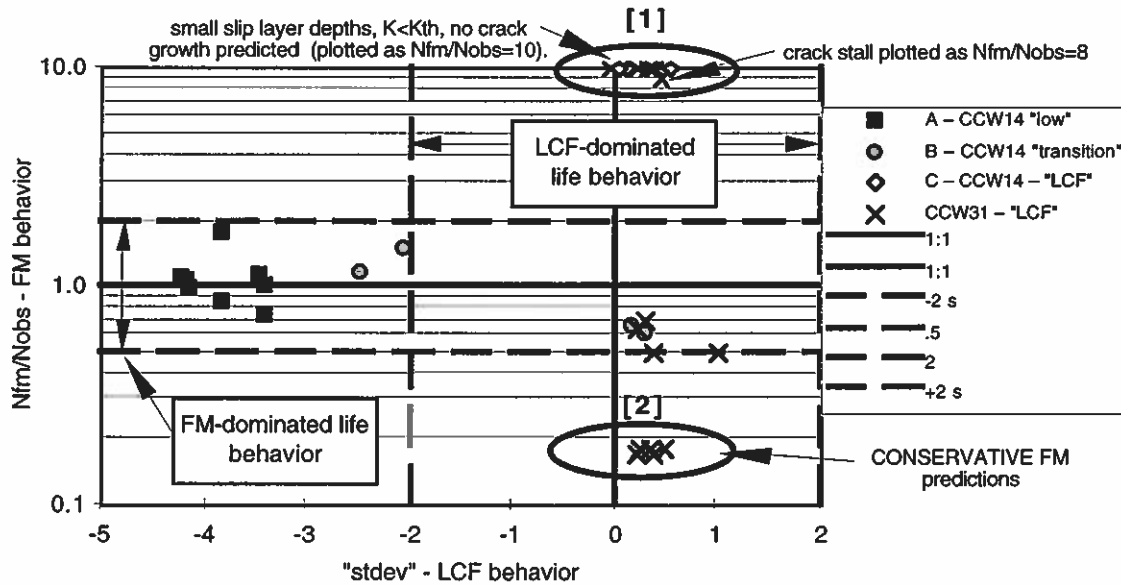


Figure 6 – Fracture Mechanics vs. LCF Domain

Specimens having low life behavior correlated with FM behavior in all cases. This suggests that sufficient strain localization was accomplished during peening to complete the crack nucleation and initiation phase, and the characteristic damage layer depth was

sufficiently great for crack propagation at the test conditions. However, there are two groups of specimens which cannot be predicted using the fracture mechanics model, which are circled and numbered on Figure 6. Group 1, near the top of the figure, consisted of specimens which had very small slip layers, resulting in calculated stress intensities (K) below the threshold value (K_{th}) required for crack growth. Group 2, near the bottom of Figure 6, consisted of specimens peened with larger shot at lower velocities. This suggests that for gentle peening conditions, the crack nucleation / initiation phase has not been completed during peening, resulting in conservative life predictions when using fracture mechanics. That is, the depth of slip does not characterize the degree of strain localization and is a necessary but not sufficient criteria for crack development. An additional criteria, shot velocity, was needed to quantify impact severity. It was not possible to find a metallurgical "tag" to characterize this condition.

The resulting Fracture Mechanics / Threshold Behavior (FM/TB) model illustrated in Figure 7 uses a dual criteria: a crack propagation threshold on the horizontal axis (which is driven by microstructural damage depth and applied stress condition), and a crack nucleation threshold on the vertical axis (an "impact severity" which is driven by total shot velocity). Both criteria must be satisfied for fracture mechanics dominated behavior to apply instead of default low cycle fatigue behavior. However, fracture mechanics can be used to provide a conservative lower bound life estimate.

Microstructure A has good life capability - low impact severity and initial crack size below the threshold value required for crack growth. Microstructure B results in "good" life capability because the initial crack size, a , is less than the threshold value required for propagation, even though the shot velocity places it in the high impact severity group. Microstructure D has "low" life capability, with severe impact condition and initial crack size greater than threshold value. These lives are well predicted using Fracture Mechanics. Microstructure C had "good" life capability. Although Fracture Mechanics calculations predict "low" life capability, it appears that additional strain localization is needed to complete macro crack development for case C (low impact severity). Use of a fracture mechanics model provides a conservative estimate of life capability for case C.

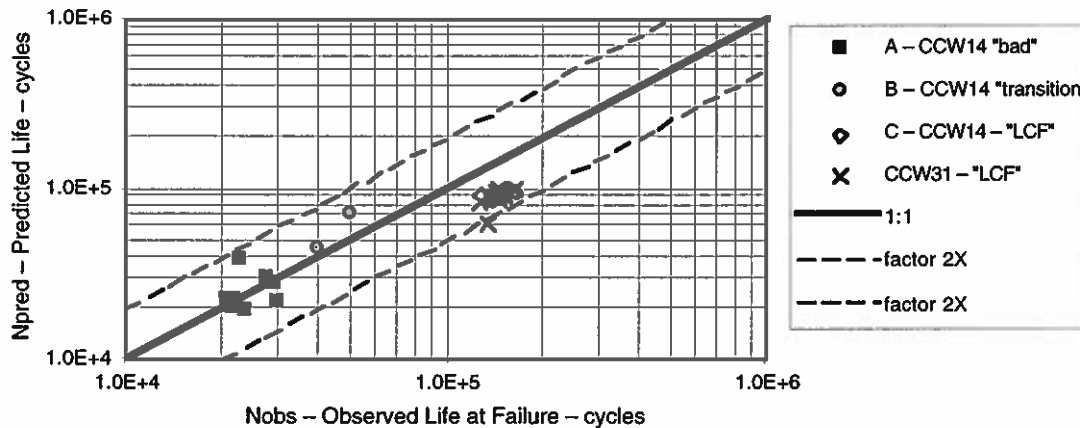
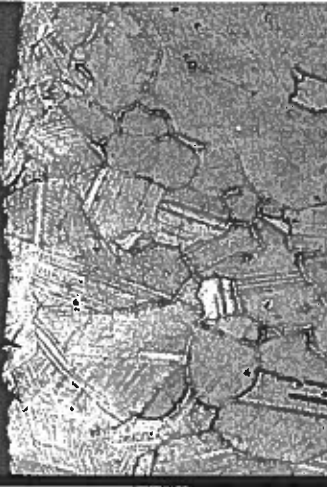





Figure 8 - Predicted Life (FM/TB model) vs. Observed Life

If a velocity threshold criteria is used to determine when to apply the fracture mechanics model, some conservatism can be removed. Referring to Figure 7, an LCF life estimate would be used for cases A and B, since fracture mechanics predicts no crack growth. For case C, a velocity threshold could be used to determine that an LCF life estimate should also be used here. Fracture mechanics predictions would be used only for case D conditions. Figure 8 shows the correlation obtained when incorporating LCF predictions for cases A-C. Note that the specimen groupings used below are consistent with those presented in Part 1 [1].

Crack NUCLEATION Threshold

HIGH Impact Severity	 <p>1) CCW14, 6A, 45°, 100%</p>	<p>“good” life</p> <p>Internal Initiations</p> <ul style="list-style-type: none"> ✓ CRACK nucleation x No crack PROPAGATION. <p>Default to LCF life.</p> <p>$V \geq 62 \text{ m/s}, \dot{\epsilon} \geq 3.4E+5,$ $a \approx .0009'' (35 \mu\text{m})$</p>	 <p>2) CCW14, 6A, 45°, 800%</p>	<p>“low” life</p> <p>SURFACE Initiations</p> <ul style="list-style-type: none"> ✓ CRACK nucleation ✓ CRACK propagation. <p>Good correlation.</p> <p>$0.5 \leq Np/Nf \leq 2.0$</p> <p>$V \geq 62 \text{ m/s}, \dot{\epsilon} \geq 3.4E+5,$ $a \approx .0021'' (83 \mu\text{m})$</p>
LOW Impact Severity	 <p>12) CCW31, 6A, 85°, 800%</p>	<p>“good” life</p> <p>Internal Initiations</p> <ul style="list-style-type: none"> x No crack NUCLEATION x No crack PROPAGATION. <p>Default to LCF life.</p> <p>$V \leq 31 \text{ m/s}, \dot{\epsilon} \leq 5.5E+4,$ $a \approx .0013'' (51 \mu\text{m})$</p>	 <p>14) CCW31, 10A, 45°, 800%</p>	<p>“good” life</p> <p>Internal Initiations</p> <ul style="list-style-type: none"> x No crack NUCLEATION ✓ Crack propagation predicted by model. <p>Conservative.</p> <p>$0.1 \leq Np/Nf \leq 1.0$</p> <p>$V \leq 39 \text{ m/s}, \dot{\epsilon} \leq 1.0E+5,$ $a \approx .0021'' (83 \mu\text{m})$</p>
		Low “K” such that $K < K_{th}, a_0 < a_{th}$		HIGH “K” such that $K > K_{th}, a_0 > a_{th}$

Crack PROPAGATION Threshold

Figure 7 – Threshold Behavior Map

SUMMARY AND CONCLUSIONS

It was observed that shot peening can reduce life capability under some circumstances. In these cases, fracture mechanics can be used to provide a lower bound estimate of life capability once a characteristic damage layer has been identified. For reduced life behavior to be observed, two criteria must be satisfied: total shot velocity must be above a threshold value (which is probably material-dependent), and the calculated stress intensity, K , must be above the threshold value, K_{th} . K is a function of crack size and stress. K_{th} is a material property, which can vary with temperature.

For René 88DT, a minimum average slip depth was used to characterize a microstructural damage layer. This layer depth was observed to increase with intensity and coverage, and was relatively independent of shot size. Incidence angle had a minor influence on slip layer depth.

In René 88DT, shot velocities above 2280 in/s (58 m/s) appeared to be sufficient to complete the crack nucleation and initiation phase. This velocity threshold may vary with alloy. To maximize life, it would be desirable to use peening conditions which stay below this threshold velocity. Intensity is a function of shot size and velocity. Larger shot will result in more gentle peening conditions than small shot at the same intensity. Near-normal (85-90°) incidence angles will result in lower velocities for a given intensity than acute angles (45°).

To apply this method to other materials, the characteristic damage layer and threshold velocity would need to be determined and substantiated with test data.

This method was developed using low cycle fatigue test data from round bars. Additional work would be needed to apply this to features such as corners.

This method appears to provide a useful lower bound estimate for life capability due to shot peening on René 88DT. This understanding can be used to select peening conditions for a specific application to maximize life capability. It can also be used to help establish robust peening process windows.

The capability to monitor shot velocity would be an important addition to shot peen process controls.

REFERENCES

- 1 Tufft, Marsha K. 1999. "Shot Peen Impact on Life, Part 1: Designed Experiment using René 88DT." *Conference Proceedings of the Seventh International Conference on Shot Peening*.
- 2 Lukás, Petr. 1996. "Fatigue crack nucleation and microstructure." *ASM Handbook Volume 19: Fatigue and Fracture*. ASM International, Materials Park Ohio. pp. 96-109.
- 3 Tufft, Marsha K. 1999. "Shot Peen Impact on Life, Part 2: Single Particle Impact Tests using Production Shot." *Conference Proceedings of the Seventh International Conference on Shot Peening*.
- 4 Tufft, Marsha K. 1997. "Development of a Fracture Mechanics / Threshold Behavior Model to Assess the Effects of Competing Mechanisms Induced by Shot Peening on Cyclic Life of a Nickel-base Superalloy, René 88DT." Ph.D. Dissertation, University of Dayton, Dayton, Ohio.
- 5 VanStone, R. contribution to Air Force final report on contract no. F33657-84-C-2047, "F101-GE-102 B-1B Update to Engine Structural Durability and Damage Tolerance Analysis Final Report (ENSIP) Volume 2." General Electric. p. 5-2-2.
- 6 Fuchs, H.O. 1981. "The Strength of Shot Peened Parts." *First International Conference on Shot Peening*, Sept. 1981, Pergamon Press: New York. pp. 323-332.
- 7 Li, J.K., Yao Mei, Wang Duo, Wang Renzhi. 1992. "An analysis of stress concentrations caused by shot peening and its application in predicting fatigue strength." *Fatigue Fract. of Engr. Mat. & Str.*, V15, N12, Dec. 1992, pp. 1271-1279.
- 8 Zukas, J.A., Theodore Nicholas, H.F. Swift, L.B. Greszczuk, D.R. Curran. 1992. *Impact Dynamics*. Krieger Publishing Company, Malabar, FL, pp. 342.